Proceedings of ASME Turbo Expo 2011
GT2011
June 6-10, 2011, Vancouver, British Columbia, Canada

GT2011-45877

CFD ANALYSIS OF A SAVONIUS ROTOR IN A CONFINED TEST SECTION AND IN OPEN FIELD

Marco Torresi
Dipartimento di Ingegneria Meccanica e Gestionale
Politecnico di Bari
Via Re David, 200, Bari 70125, Italy
Tel: +39-080-596-3577, Fax: +39-080-596-3411
Email: m.torresi@poliba.it

Bernardo Fortunato
Dipartimento di Ingegneria Meccanica e Gestionale
Politecnico di Bari
Via Re David, 200, Bari 70125, Italy
Tel: +39-080-596-3223, Fax: +39-080-596-3411
Email: fortunato@poliba.it

Giuseppe Pascazio
Dipartimento di Ingegneria Meccanica e Gestionale
Politecnico di Bari
Via Re David, 200, Bari 70125, Italy
Tel: +39-080-596-3221, Fax: +39-080-596-3411
Email: pascazio@poliba.it

Sergio Mario Camporeale
Dipartimento di Ingegneria Meccanica e Gestionale
Politecnico di Bari
Via Re David, 200, Bari 70125, Italy
Tel: +39-080-596-3627, Fax: +39-080-596-3411
Email: camporeale@poliba.it

ABSTRACT

Aim of this paper is to provide a deep insight into the dynamic behavior of the flow through a Savonius rotor by means of computational fluid dynamics (CFD). The analysis is carried out solving the incompressible Unsteady Reynolds Averaged Navier-Stokes equations, providing fundamental information concerning the complex unsteady flow field in and around the rotor. The motivation for employing a numerical approach relies on the consideration that detailed analysis of wind turbines, aiming to improve their design, cannot be easily performed by means of experimental full-scale field-testing due to the lack of control on the test conditions. At the same time, few are the wind tunnels where large turbine prototype testing is possible, so that experimental tests are usually carried out inside wind tunnels having dimensions comparable with those of the prototype. Moreover, if the available wind tunnel has a confined test section, the turbine performance could be quite different from those expected in open field.

Therefore, in this paper, the turbine is firstly supposed to operate in open field and then in a bounded test section, in order to analyze the effect of flow confinement and to correlate the turbine performance in open field with experimental results obtained from prototypes tested in small wind tunnels of assigned blockage.

KEYWORDS

U-RANS, VAWT, wind tunnel

NOMENCLATURE

a	[m]	= rotor shaft diameter
A	[m^2]	= test section area
AR	[-]	= H/d aspect ratio
A_s	[m^2]	= $D\ H$ rotor swept area
b	[-]	= $(e-a)/d$ = overlap ratio
B	[m]	= equivalent tunnel width for 2D simulations
C_P	[-]	= $T\omega/(1/2\ \rho\ V_{inf}^3\ A_s)$ = power coefficient
C_m	[-]	= $T/(1/2\ \rho\ V_{inf}^2\ A_s\ R)$ = torque coefficient
d	[m]	= nominal bucket diameter
D	[m]	= $2d-e$ = rotor diameter
D/Dt	[1/s]	= substantial derivative
D_d	[m]	= end-plate diameter

D_s	[m]	= central shaft diameter
e	[m]	= rotor overlap
f	[Hz]	= frequency
H	[m]	= rotor height
N	[-]	= number of buckets
R	[m]	= $D/2$ = rotor tip radius
Re	[-]	= $V_{inf}D/\nu$ = Reynolds number
p	[Pa]	= gauge static pressure
P	[W]	= $T\omega$ = shaft power
s	[m]	= bucket thickness
s_d	[m]	= end-plate thickness
St	[-]	= $f\,D/V_{inf}$ = Strouhal number
t	[s]	= time
T	[Nm]	= shaft torque
T_p	[s]	= time period
U_{tip}	[m/s]	= ωR = tip speed
u_j	[m/s]	= j^{th} component of the fluctuating velocity
U_j	[m/s]	= j^{th} component of the mean velocity
V_{inf}	[m/s]	= free stream velocity
β	[m]	= A_s/A = bucket radius
Δt	[s]	= time step
λ	[-]	= U_{tip}/V_{inf} = tip speed ratio
ν	[m^2/s]	= kinematic viscosity
ρ	[kg/m^3]	= air density
θ	[deg]	= bucket rotation angle (Fig. 1)
ω	[rad/s]	= rotational speed

INTRODUCTION

Nowadays, the main part of the World electric consumption is fueled by: coal/peat (41.0%), gas (21.3%), nuclear (13.5%), and oil (5.5%) [1]. The maximum limit of fossil fuel production seems to be already reached and fossil fuel depletion (at actual price) seams unavoidable in the next decades. Furthermore, fossil fuels are the main sources of pollutant emissions (first of all CO_2, NO_x, and particulate).

One way to face up these problems is to consider the use of renewable energy sources. Among renewable sources, wind energy seems to have the lower global impact on the environment, especially taking into account applications of distributed production. Actually, the technically available global wind energy is estimated to be more than twice the World energy demand.

The current trend in wind turbine design goes towards opposite directions: at one side, bigger and bigger rotors are built up especially for off-shore applications (up to 5 MW), even though the initial exponential growth is experiencing a slow down and currently there is an increasing volume supply in the 1.5 - 3 MW range [2]; on the other side, small wind turbines (up to 100 kW) are gaining greater importance.

Small wind turbines are thought to solve local needs directly on site by means of stand alone systems. The main reason for developing such a technology is the possibility to install small aero-generators in sites where wind power is high enough but very concentrated, hence not energetically useful for big wind farms. Then the diffusion of small wind turbines can imply a more rational use of the wind energy all over the territory. Hence, small models are not alternative but complementary to big ones.

If the market of big wind turbines is dominated by Horizontal Axis Wind Turbine (HAWT), in the market of small wind turbines there is more space for other options and particularly for Vertical Axis Wind Turbine (VAWT). Among small VAWTs, here the attention is focused in particular on the Savonius rotor. Despite Savonius rotors have lower performance compared to HAWT, there is a renewed interest because of the commercialization of Windside rotors, which can be considered directly derived from Savonius rotor by means of a twisting along its rotation axis. Like other VAWTs, the Savonius rotor has the invaluable advantage to be able to capture wind energy independently of the wind direction and it is characterized by a high starting torque. Using a specific comparison method (namely the L-σ criterion), Menet *et al.* [3] have shown that Savonius rotors are extremely more resistant to mechanical stresses than any other fast running wind machine. These characteristics make the Savonius rotors particularly suitable for coupling with pumps. In fact, authors like Rabah & Osawa [4], Valdès & Raniriharinosy [5], Valdès & Ramamonjisoa [6] have focused their attention on this application, aiming at developing wind pumping devices of low technicality suitable for poor countries.

In order to have a better understanding of the turbine performance, several authors carried out tests on controlled environment by means of subsonic wind tunnels. Blackwell *et al.* [7] carried out an extensive experimental campaign on two and three bucket Savonius rotors, in the Vought Corporation System Division low speed wind tunnel, at different Reynolds numbers. Lately, Kamoji *et al.* [8] focused their attention on the effects of the overlap ratio and the end tip configurations (blunt or round edge). New Savonius configurations have also been considered and tested in low speed wind tunnels. In order to obtain a smooth shaft torque coefficient, Menet [9] proposed a double-stepped Savonius rotor and Hayashi *et al.* [10] investigated a three-stepped Savonius rotor. In order to further smooth the turbine operation and trying to improve its efficiency, twisted buckets have been also taken into account (e.g. Grinspan *et al.* [11], Saha & Rajkumar [12]). Gupta *et al.* [13] focused their attention on the coupling of a Savonius machine with a Darrieus rotor. However wind tunnel and field tests give only global performance without a thorough description of the complex flow structures in and around the rotor. In order to analyze the vortex formation downstream of the rotor, Benghrib *et al.* [13] registered a film from visualization in a water channel with dye emitted from the center of the rotor. Also numerical simulations have been carried out trying to give a better understanding of the fluid-dynamic pattern in and around the rotor. A pioneer in this approach is Fujisawa [15] who presented both experimental and numerical results. In particular, he carried out measurements of phase averaged velocity distribution by means of Particle Image Velocimetry (PIV) and compared the flow pattern with numerical calculation by means of a discrete vortex method. However, the reproduction of the flow field around a stationary rotor, by his own judgment, was poor. Later on, Kawamura *et al.* [16] investigated numerically the Savonius rotor performance using a domain decomposition method. Menet & Bourabaa [17] and Menet & Cottier [18] carried out extensive parametric investigations on Savonius rotors by means of numerical computations relying on the Navier-Stokes equation solver Fluent, which led them to precise the nature of the flow and to determine its aerodynamic behavior.

Recently, some researchers focused their interest on combining multiple Savonius turbines in the horizontal plane in order to produce extra power, by means of the interaction between the flow fields around the individual turbines [19]. Cochran *et al.* [20] proposed a totally integrated approach based on multiple design tools: CFD computation; reduced-scale testing; and full-scale field testing. This “three-tiered” approach allowed them to significantly improve the power performance of their rotor model. In their CFD analysis, D’Alessandro *et al.* [21] take into account the action of the flow on the rotor, which is controlled at constant torque, and hence experience a continuous angular speed variation.

Validation of numerical results relays on accurate experimental results. However the assessment of experimental field testing controlling all the boundary conditions is not easy at all. At the same time, it is extremely expensive to develop and manage huge wind tunnels in order to test full scale turbine prototypes. Commonly, closed loop subsonic wind tunnel can be found where only small scale prototypes can be actually tested. In order to be able to measure significant torque and power values, the prototype dimensions should be assessed to the highest value compatible with the cross test section. However the flow confinement due to the section walls greatly alters the rotor performance with respect to the open field conditions. For this reason, the authors propose a new approach which strongly relay on CFD, solving the incompressible Unsteady Reynolds Averaged Navier-Stokes (U-RANS) equations and providing fundamental information concerning the complex unsteady flow field in and around the rotor. The CFD simulations are firstly carried out in open field, then the same rotor is simulated inside a confined domain, reproducing typical small wind tunnel conditions. In such a way, the authors aim to put in evidence the effect of flow confinement and to give a tool to develop correlations able to predict the turbine performance in open field starting from experimental data available from prototypes tested in wind tunnels of assigned blockage.

THE SAVONIUS ROTOR

The Savonius Rotor is a VAWT ideated by the Finnish engineer S.J. Savonius in 1922. This VAWT is characterized by a very simple geometry and, from an aerodynamic point of view, it is mainly a drag-driven device consisting of two or three buckets generally of half cylindrical shape (Fig. 1).

In the conventional configuration with two semicircular buckets, each one is characterized by a nominal diameter, d, and a height, H. In order to improve the rotor performance, the two buckets present an overlap, e. The model under investigation has a central shaft between the buckets, which are hold by two end-plates of diameter D_d.

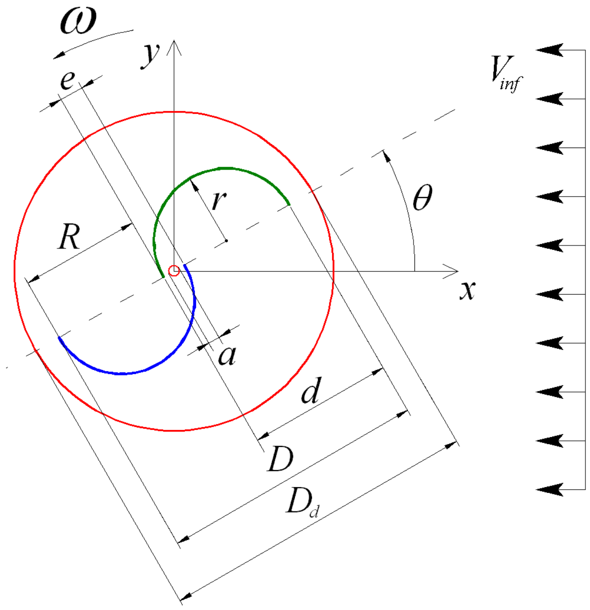

Fig. 1 Schematic of a two bucket Savonius rotor

The Savonius turbine efficiency, which is actually relatively low, is affected by the following main geometrical parameters:

- the aspect ratio, AR, which represents the ratio between the rotor height, H, and the bucket diameter, d;
- the overlap ratio, b;
- the end-plate diameter D_d;
- the bucket thickness, s;
- the number of buckets, N.

A fundamental operating parameter is the tip speed ratio, λ, namely the ratio between the tip speed velocity, $U_{tip} = \omega R$, and the free stream velocity, V_{inf}.

Relaying on a long experimental activity, a particular geometry has been defined, bringing to the so called optimum Savonius rotor [22], for which the overlap ratio, b, is equal to 1/6 and the aspect ratio, AR, is equal to 4.

Global turbine performance is usually given in non-dimensional form by means of the power coefficient, C_P, which represents the fraction of power extracted from the available wind power. When the starting torque is considered, but not only in this case, the turbine performance needs to be expressed in term of torque coefficient, C_m.

Fig. 2 Savonius rotor under investigation

The Savonius rotor prototype under investigation (Fig. 2) actually doesn't respect the optimum design, since the aim was to maximize the torque and to limit the flow blockage. To improve the overall stiffness of the rotor, a central shaft is applied, which then reduces the actual overlap. The buckets are obtained by splitting longitudinally a PVC pipe (d = 200 mm; PN6; s = 5.1mm). PVC is particularly suited for this application due to its low specific weight, a good mechanical strength, a relatively low cost and ease of machinability. The overlap is e = 65 mm, whereas the central shaft diameter is D_s = 20 mm. In order to ensure that the prototype is at the centre of a 1x1 m^2 test section and taking into account the space needed for the supports, the rotor height has been fixed to H = 412 mm. The aluminum end plates have a diameter D_d = 360 mm and they are tighten one to each other not only by means of a blockage screwed to the rotor shaft but also by means of two small steel beams (characterized by a 5mm diameter) placed in front of the external end buckets.

COMPUTATIONAL DOMAINS

In order to perform the 2D numerical simulations, two different computational domains were considered: one for the open field simulations; the other for the confined ones. In particular, for the latter case, a reference cross section area equal to 1x1 m^2 is supposed. In the former case (Fig. 3), the computational domain is circular, 15 meters in diameter, hence about 40 times the rotor diameter, allowing the complete development of the vortices in the wake. The entire computational domain was discretized by means of about 130000 cells, refined moving towards the rotor. In order to accurately simulate the flow around the turbine, the computational domain was divided into two parts: an external fixed zone and an internal circular zone rotating together with the Savonius rotor.

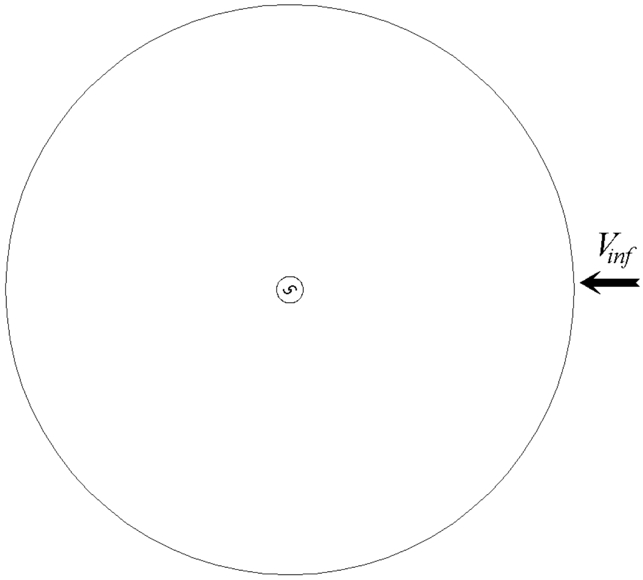

Fig. 3 Open field computational domain

For the external zone a structured mesh was used, coarsening the cells from the interface up to far field. Instead, for the internal moving zone, a multi-block hybrid mesh was used (Fig. 4): close to the rotor buckets and the shaft (Fig. 5), a structured grid was used in order to accurately simulate the boundary layers (the first cell height, equal to $2 \cdot 10^{-5}$ m, was designed in order to have, during all the simulations, y^+ values lower than 1); whereas the remaining part was meshed with unstructured triangular cells having size equal to 0.0025 m near the bucket surfaces and reaching a maximum cell size equal to 0.009 m at the interface with a growth rate of 1.15.

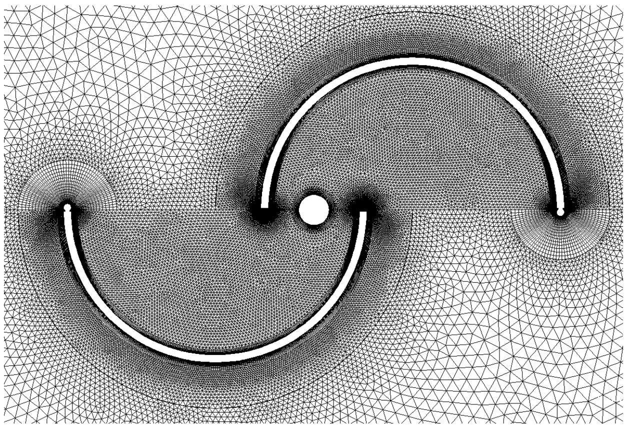

Fig. 4 Grid detail around the buckets and the rotor shaft

For the Savonius rotor operating inside a wind tunnel, the computational domain needs to be modified in order to take into account the actual confinement due to the wind tunnel walls.

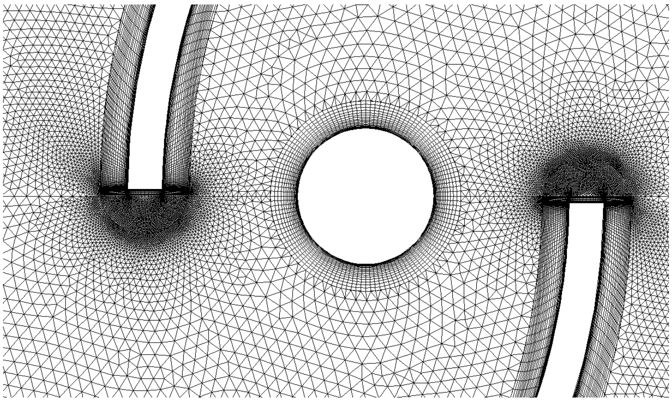

Fig. 5 Structured grid around the rotor shaft

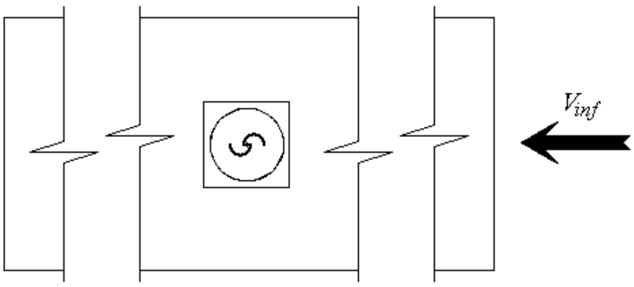

Fig. 6 Confined computational domain

The rotor is placed at the centre of a 10 m long duct allowing the complete development of all vortices in the wake (Fig. 6). The transversal width of the domain, B, was set to 2.5 m, even if the reference wind tunnel has a cross test section 1x1m^2. The actual 2D domain is to be chosen wider than the reference wind tunnel section in order to maintain the same blockage factor as the one pertaining to the reference wind tunnel. The rotor swept area, A_s, is equal to 0.1359 m^2 and the cross test section is 1m^2 giving an actual blockage factor, β, equal to 0.1359. Therefore, moving from the 3D experimental to the 2D numerical configuration, there is no more a geometric similitude but a functional one. In fact, when the actual three-dimensional airflow invests the rotor inside the closed wind tunnel, the streamlines partially interact with the rotor and partially bypass it. When 2D simulations are performed, the streamlines can actually bypass the rotor only sideway, as if the rotor height was exactly equal to the wind tunnel height, implying that a greater number of streamlines ought to interact with the rotor, hence obtaining a greater energy extraction than actually obtained. In order to restore similar operating conditions the authors suggest to enlarge the tunnel width when performing the 2D simulations so as to recover the same blockage factor.

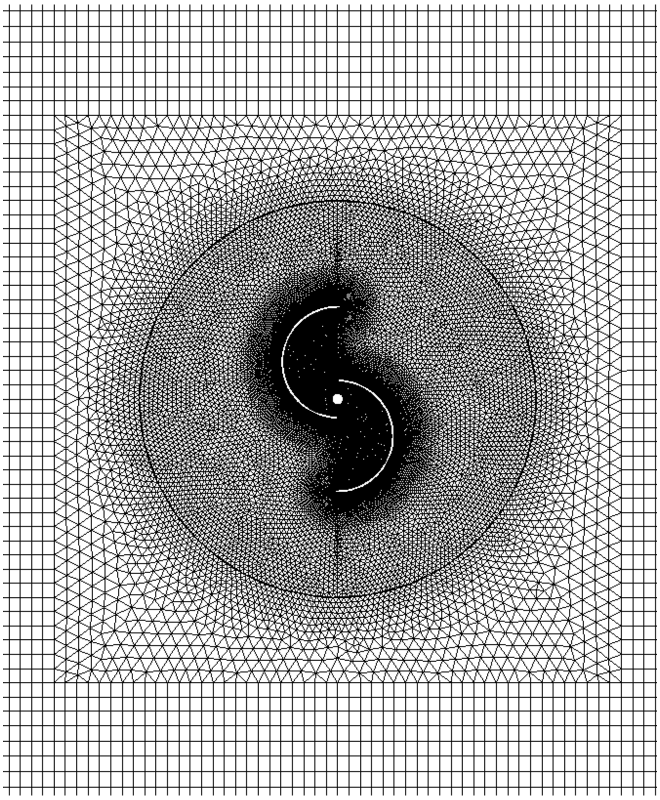

Fig. 7 Detail of the transition zone

The confined computational domain comprises now a total of 156000 cells. According to the sliding mesh technique, three cell zones have been considered: a cylindrical internal zone, which is identical to the previous one and rotates together with the VAWT; a rectangular confined fixed zone; finally a fixed squared transition zone between the previous two. The transition zone is discretized by means of an unstructured mesh (Fig. 7), whereas the confined fixed zone was discretized by means of a multi-block structured grid. The mesh was also refined closed to the tunnel walls (first cell height equal to $5 \cdot 10^{-5}$ m), in order to accurately simulate the boundary layer growth.

CFD MODEL

The commercial CFD code Fluent® ver. 6.3.26 has been used to carry out the numerical simulations. The mass conservation equation together with the Unsteady Reynolds-Averaged Navier-Stokes (U-RANS) equations for incompressible flows:

$$\frac{\partial U_j}{\partial x_j} = 0$$
$$\frac{DU_j}{Dt} = -\frac{1}{\rho}\frac{\partial p}{\partial x_j} + \left[\upsilon \left(\frac{\partial U_i}{\partial x_j} + \frac{\partial U_j}{\partial x_i} \right) - \overline{u_i u_j} \right], \qquad (1)$$

are discretized by means of a finite volume approach, with respect to a fixed reference frame.

The implicit segregated version of the solver is employed. The pressure-velocity coupling is achieved by means of the SIMPLE (Semi-Implicit Method for Pressure-Linked Equations) algorithm. The convective terms are discretized using a second order accurate upwind scheme, and pressure and viscous terms are discretized by means of a second order accurate centered scheme. A second order implicit time formulation is also used. Closure for turbulence effects in the RANS equations has been achieved by means of the standard k-ω model with the low-Reynolds correction [23]. The Reynolds stress tensor is then related to the mean strain rate tensor according to the Boussinesq approach. Actually the governing equations are solved in two different computational domains: one rotating together with the Savonius rotor; the other fixed. The sliding mesh model allows the computation of the flux across the two non-conformal interface zones.

RESULTS

The flow simulations have been performed using the following boundary conditions: at the inlet section a uniform wind speed (velocity inlet) equal to 5 m/s with a turbulent intensity equal to 2% and a turbulent length scales of 1% of the rotor diameter; at the outlet section a fully developed flow condition (outflow); all the solid parts of the rotor (buckets and rotor shaft) are considered wall with a relative velocity equal to zero with respect to the internal rotating domain and the no-slip condition has been taken into account. The angular velocity has been assigned to the internal rotating domain according to the corresponding tip speed ratio considered (λ = 0.25, …, 1.75, $\Delta\lambda$ = 0.25).

The number of iterations per time step is 100, which allows to have values of the residuals less than 10^{-8}. For every simulation, the time step, Δt, is set in such a way to perform an angular rotation, $\Delta\theta$, equal to 1 deg for each time step.

In order to reach solution convergence, at least 10 complete rotor revolutions have been performed verifying the periodicity of the solution superposing the torque coefficient of the two last revolutions (see, for example, Fig. 8).

The simulations were carried out on a PC with a dual-core processor Intel© Core™ 2 Duo T7500 (2.2 GHz per unit, 4 MB cache) and a 2 Gigabyte DDR2 RAM. The time required to perform each complete simulation was about 5 days.

Open-field simulations

In order to describe the main features of the flow behavior in and around the Savonius rotor, the simulation carried out at λ = 0.75 is considered. During the iterations, the torque coefficient was registered at each time step. The iteration process was terminated when the solution has reached periodicity. For instance Fig. 8 provides the torque coefficient, C_m, versus the rotor angular position, θ, for the two last revolutions. Even if the rotor is characterized by a geometrical symmetry of 180°, this is not the case for the torque coefficient, which reveals a slightly but significant lack of symmetry; in fact, the actual angular period is equal to 360°. At the same time, the polar diagram of the torque coefficient is provided in Fig. 9, evidencing the typical bilobed shape.

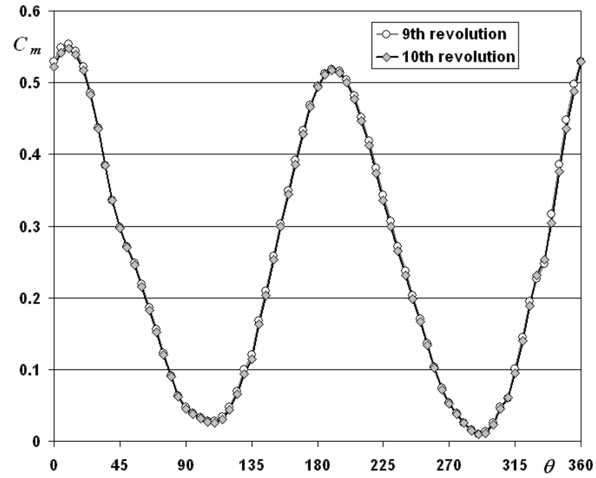

Fig. 8 Torque coefficient at λ = 0.75 – last 2 revolutions

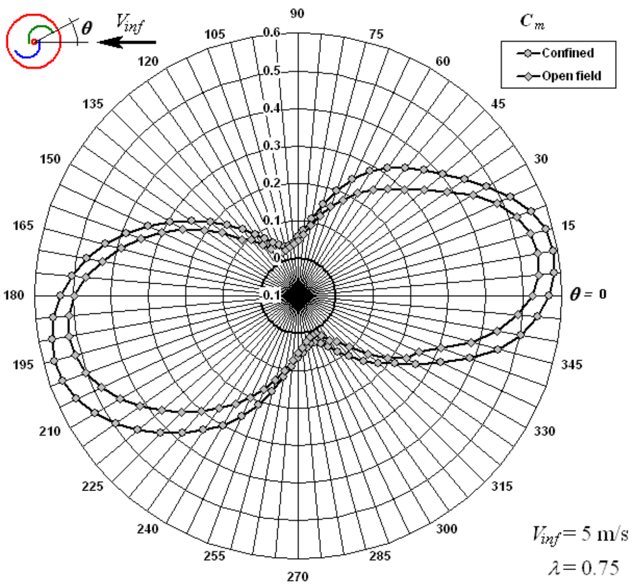

Fig. 9 Polar diagrams of torque coefficient at λ = 0.75; V_{inf} = 5 m/s

At the tip speed ratio under investigation, the rotor experiences the maximum torque coefficient at θ = 10° and 190°, whereas the minimum torque coefficient is achieved at θ = 110° and 290°. When the buckets are almost perpendicular with respect to the free stream velocity, even if the advancing bucket is giving the highest torque contribution, the returning bucket is actually giving its strongest adverse contribution. This could be particularly evidenced by looking at the pressure field around the Savonius rotor (Fig. 10).

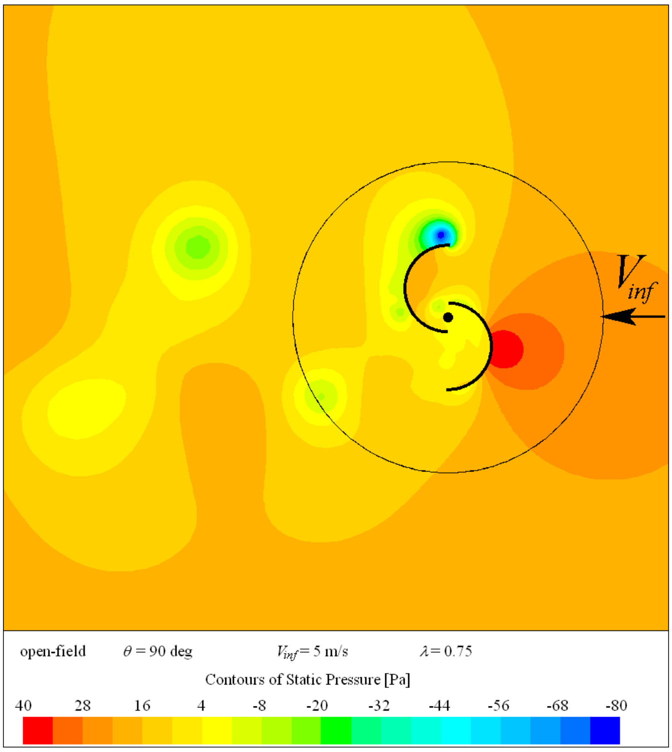

Fig. 10 Contours of static pressure – open field simulation at λ = 0.75; V_{inf} = 5 m/s; θ = 90 deg

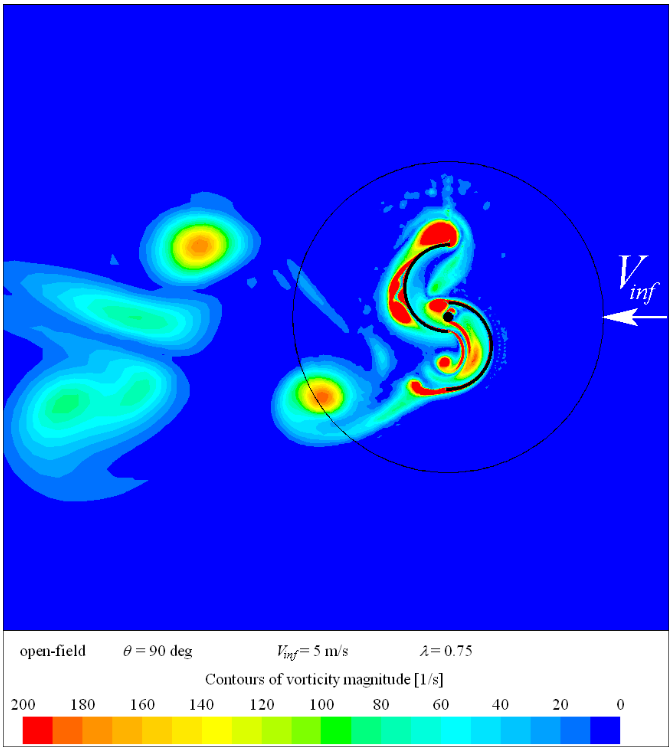

Fig. 11 Contours of vorticity magnitude – open field simulation at λ = 0.75; V_{inf} = 5 m/s; θ = 90 deg

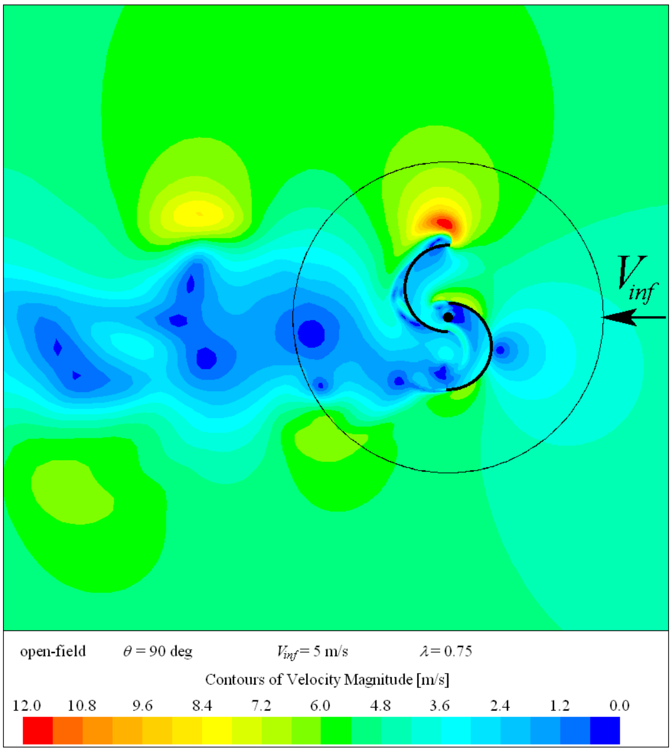

Fig. 12 Contours of velocity magnitude – open field simulation at λ = 0.75; V_{inf} = 5 m/s; θ = 90 deg

Conversely, when the buckets are almost aligned with respect to the free stream velocity, the advancing bucket gives a minimum resistant contribution to rotation; whereas the returning bucket, due to the flow passing through the overlap passage, experiences a positive lifting action maximizing the torque coefficient.

As previously mentioned, the torque coefficient is not characterized by an angular periodicity equal to 180°. The main reason for such a behavior is to be found in the complex interaction of the vortex shedding with the rotating buckets, as shown by the contours of the vorticity magnitude (Fig. 11). In particular the vortices interact with the bucket surfaces differently every 180°. It is worth noting another peculiar behavior of the flow around a Savonius rotor: actually, the rotor wake is not perfectly symmetrical with respect the rotor axis (Fig. 12). The streamwise velocity is slightly higher in the semi-plane of the advancing bucket, thus showing a behavior very similar to that encountered in the flow around a rotating cylinder.

When the tip speed ratio changes the main flow feature remains almost the same. However some differences needs to be put in evidence. These differences determine modifications of the polar diagrams of the torque coefficient (Fig. 13), which in turns explains the typical behavior of the characteristic curves of the Savonius rotor (Fig. 14).

As the tip speed ratio increases the bilobed shape of the torque coefficient polar diagram is markedly intensified and shows a counterclockwise rotation. Moreover, torque coefficient maxima slightly decrease, whereas minima collapse showing extremely high negative values ($C_{m,min}$ = -0.7 at $\lambda = 1.75$). The negative torque contribution increases together with the increase of the tip speed ratio, which determines the almost linear decay of the averaged torque coefficient with the increase of the tip speed ratio.

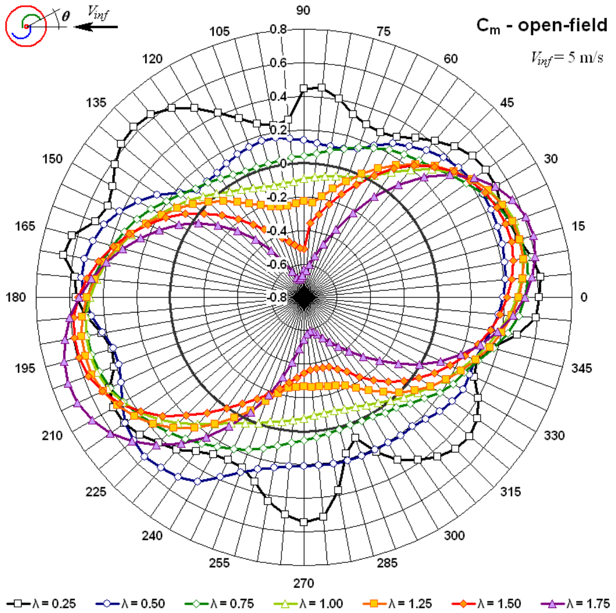

Fig. 13 Polar diagrams of torque coefficient – open field

Conversely, when the tip speed ratio decreases, another feature needs to be evidenced: the torque coefficient polar diagram loses a regular bilobed shape and shows a more complex behavior. In order to explain such a behavior, the contours of vorticity magnitude at two different tip speed ratio, $\lambda = 0.50$ (Fig. 15) and $\lambda = 1.25$ (Fig. 16) respectively, may help.

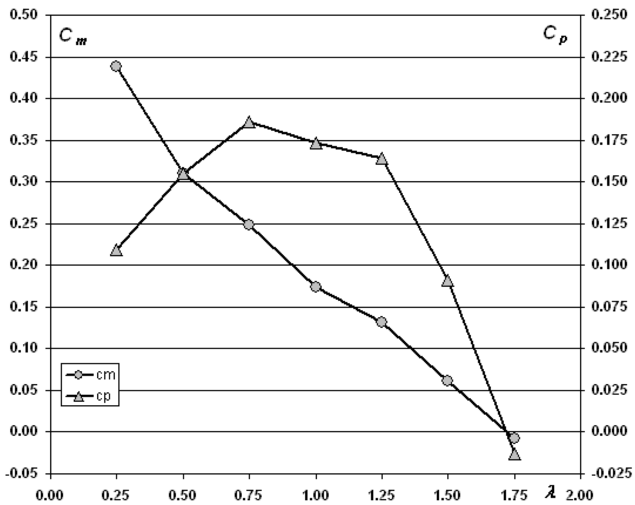

Fig. 14 torque and power coefficients vs. tip speed ratio

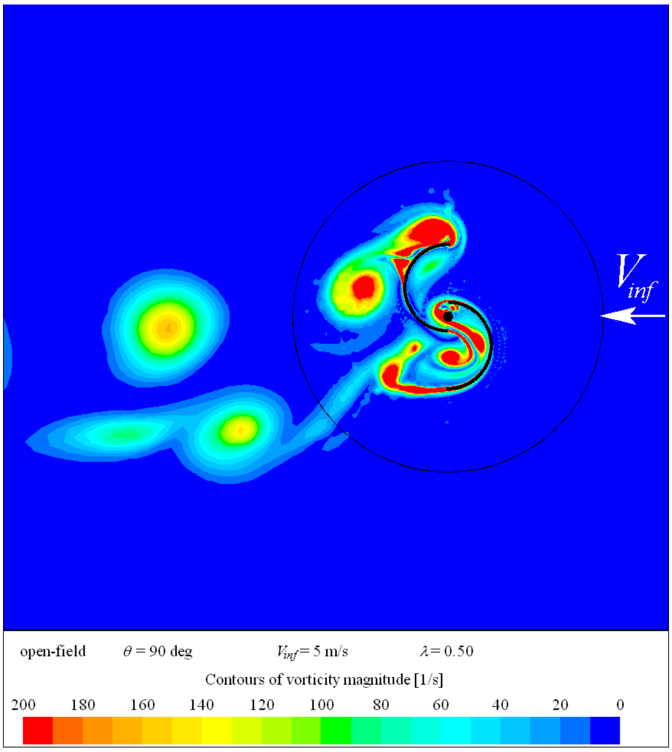

Fig. 15 Contours of vorticity magnitude – open field simulation at $\lambda = 0.50$; $V_{inf} = 5$ m/s; $\theta = 90$ deg

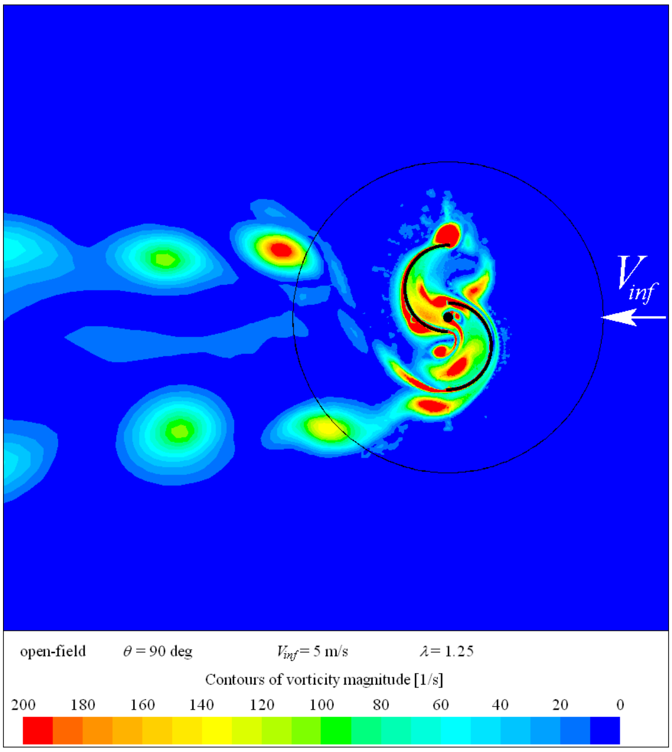

Fig. 16 Contours of vorticity magnitude – open field simulation at $\lambda = 1.25$; $V_{inf} = 5$ m/s; $\theta = 90$ deg

At λ = 0.50, due to the low rotational speed, the vortex generated from the advancing bucket can be firstly shed and then again interact with it modifying the rotor performance; whereas at λ = 1.25, due to the higher rotational speed, the vortex generated from the advancing bucket is squished on the advancing bucket itself, giving a smoother torque coefficient behavior.

Confined simulations

In order to investigate the influence of the test section side walls on the performance of the Savonius rotor, 2D numerical simulations were performed within a confined computational domain (Fig. 6). As previously mentioned, in order to preserve the same flow confinement characteristics, the 2D computational domain is actually larger than the reference wind tunnel but with the same blockage factor.

The pressure contours (Fig. 17) show the following minor differences with respect to those of the open field case: (i) the high pressure region at the convex side of the returning bucket is wider; (ii) a higher pressure value is also registered at the concave side of the advancing bucket. Globally, the two effects determine a higher torque coefficient in the confined case.

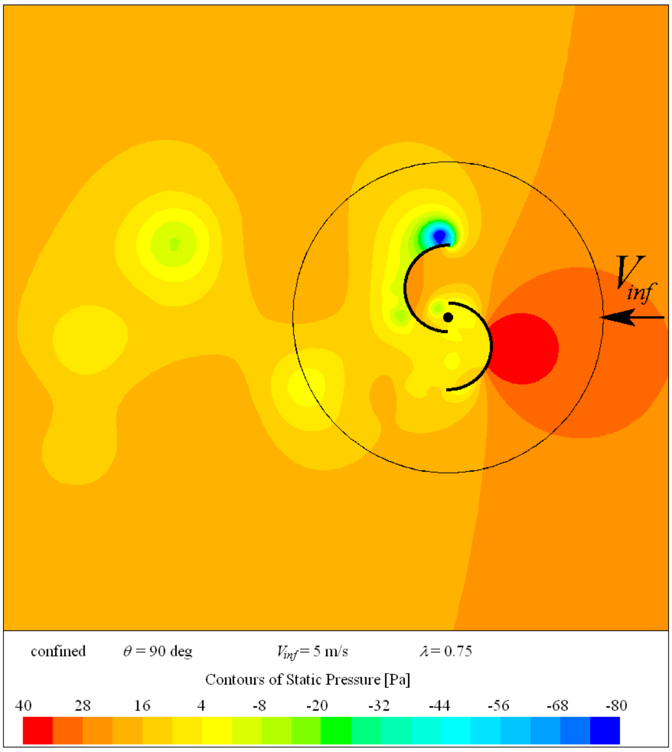

Fig. 17 Contours of static pressure – confined simulation at λ = 0.75; V_{inf} = 5 m/s; θ = 90 deg

Looking at the vorticity magnitude distribution (Fig. 18), the attention has to be focused on the overlap region inside the Savonius rotor: due to the confinement a larger amount of mass flow rate passes through the bucket overlap, as evidenced by greater vortical structures shed both by the rotor shaft and the trailing edge of the advancing bucket.

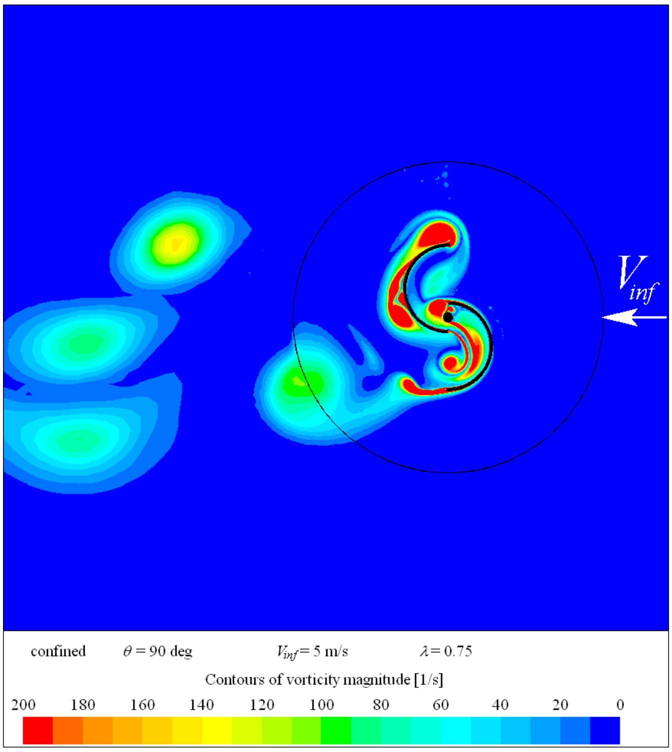

Fig. 18 Contours of vorticity magnitude - confined simulation at λ = 0.75; V_{inf} = 5 m/s; θ = 90 deg

Comparing the polar diagrams of the torque coefficient at λ = 0.75, for both the confined and open field cases (Fig. 9), it is evident that in the former case the rotor performance are constantly higher than in the latter case. As mentioned before, the reason is basically due to the confinement effect of the tunnel side walls, which force a greater amount of flow to interact with the Savonius rotor. This behavior is preserved at all the tip speed ratios characterized by a positive rotor power contribution (Fig. 19). Close to the maximum power coefficient (λ ranging from 0.75 up to 1.25) an increase ranging from 15% up to 20% is observed.

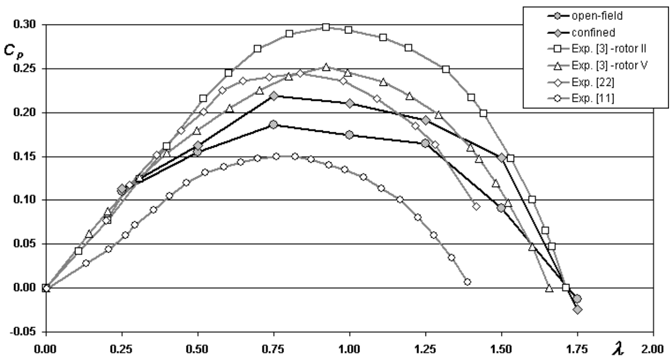

Fig. 19 Power coefficient vs. tip speed ratio

The performance of the Savonius rotor under investigation are well in the range of typical configuration available in literature (Fig. 19). In particular, since our rotor doesn't respect the optimum design, it shows lower performance with respect to the "optimum" Savonius rotor (indicated in Le Gourieres [22] as Rotor II), which reaches $C_{p,max}$ = 0.3. However, when the overlap ratio is increased to 0.43 (Rotor V [22]) the $C_{p,max}$ decreases to 0.25. On the other hand, the $C_{p,max}$ for the rotor studied by D'Alessandro *et al.* [21] is equal to 0.244. Moreover it is possible to find Savonius rotor with lower performance such as the one tested by Hayashi *et al*. [10] for which the $C_{p,max}$ is equal to 0.15. The wide range of performance can be traced back to the differences in the geometries of all these rotors.

In order to evidence the confinement effect, it is possible to consider the streamwise velocity distributions downstream of the rotor (y = 3m from the rotor axis) for both the confined and open field cases (Fig. 20). In both cases a velocity reduction with respect to the free stream value is observed in the turbine wake; however, in order to preserve the mass flow rate, the velocity outside the wake needs to accelerate: in the open field case, the velocity is actually only slightly higher than the free stream velocity, whereas, in the confined case, the velocity is at least a 10% higher except in the side wall boundary layers.

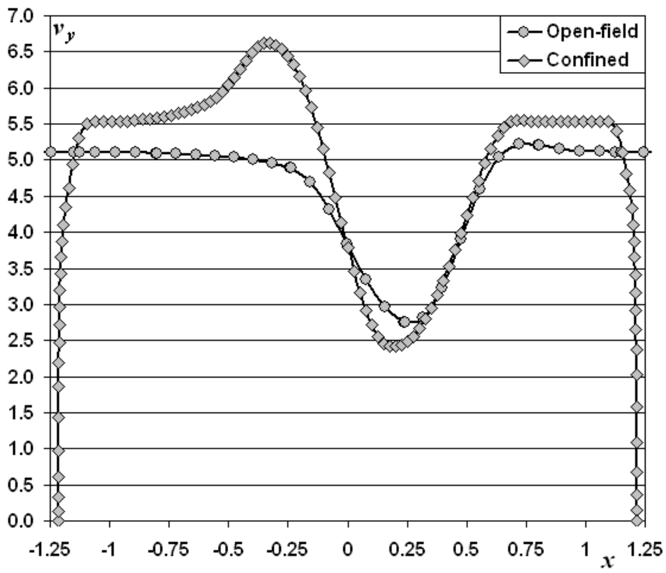

Fig. 20 Streamwise velocity, v_y at y = 3m and θ = 90°

The polar diagrams of the torque coefficient (Fig. 21) show the same behavior as those of the open field case: when the tip speed ratio increases, the bilobed shape of the torque coefficient polar diagram is intensified, torque coefficient maxima remain very close one to each other, whereas minima collapse showing extremely high negative values ($C_{m,min}$ = -0.8 at λ = 1.75).

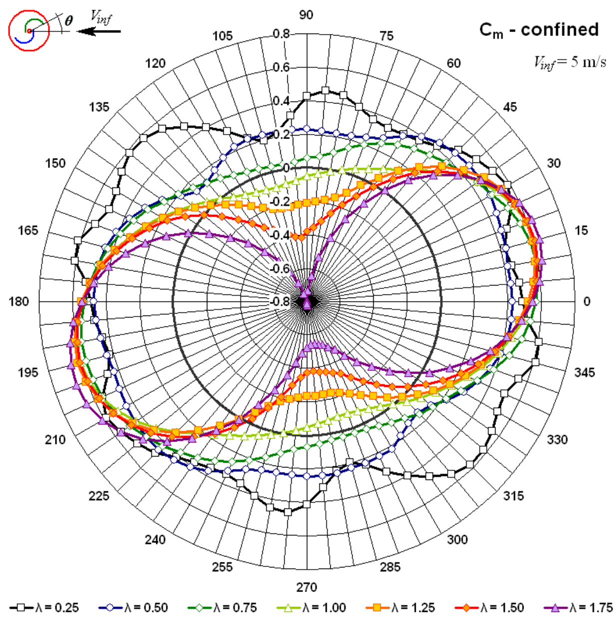

Fig. 21 Polar diagrams of torque coefficient – confined

CONCLUSIONS

In this work, the performance of the Savonius rotor prototype developed at the Politecnico di Bari has been analyzed by means of a CFD approach. 2D simulations have been carried out considering the VAWT rotating both in an open field and in a confined domain representing a small wind tunnel.

By means of accurate CFD simulations, it was possible to put in evidence that the Savonius rotor experiences significant dynamic effects. In fact, the polar diagram of the torque coefficient is markedly affected by the value of tip speed ratio resulting in the typical averaged torque coefficient behavior, which decreases almost linearly with the tip speed ratio.

Finally it has been shown that, due to the confinement effect, which forces a greater number of streamline to interact with the rotor inside the wind tunnel with respect to the open field case, the performance in the former case are actually higher, providing an increase up to 20% near the maximum power coefficient (λ ranging from 0.75 up to 1.25).

ACKNOWLEDGMENTS

We would like to express thanks to Luca Sciacovelli for his invaluable help in carrying out the numerical simulations.

REFERENCES

[1] "Key World Energy Statistics 2010", IEA 2010.

[2] "The Economics of Wind Energy", a report by the European Wind Energy Association, March 2009

[3] Menet J.-L. Valdès L.-C. Ménart B., 2001, “A comparative calculation of the wind turbines capacities on the basis of the L-σ criterion”, Renewable Energy, 22: 491-506
[4] Rabah K.V.O., Osawa B.M., 1996, “Design and field testing of Savonius wind pump in East Africa”, Int. J. Amb. En., 17-2:89-94
[5] Valdès L.-C., Raniriharinosy K., 2001, “Low technical pumping of high efficiency”, Ren. Energy, 24:275-301.
[6] Valdès L.-C., Ramamonjisoa B., 2006, “Optimised design and dimensioning of low-technology wind pumps”, Renewable Energy, 31:1391–1429
[7] Blackwell B.F., Sheldahl R.E., Feltz L.V., 1977, “Wind tunnel performance data for two-and three-bucket Savonius rotors”, Sandia National Lab., SAND-76-0131
[8] Kamoji M.A., Prabhu S.V., Kedare S.B., 2006, “Experimental Investigations on the Effect of Gap Ratio and End Tip Condition on the Static Torque in a Conventional Savonius Rotor”, in Proceedings of the National Conference on Advances in Energy Research, 4th & 5th, December, IIT-Bombay
[9] Menet J.-L., 2004, “A double-step Savonius rotor for local production of electricity: a design study”, Renewable Energy, 29: 1843–1862
[10] Hayashi T., Li Y., Hara Y., Suzuki K., 2004, “Wind tunnel tests on a three-stage out-phase Savonius rotor”, in Proceeding of the European Wind Energy Conference, London, 22-24 November 2004
[11] Grinspan A.S., Suresh Kumar P., Saha U.K., Mahanta P., Ratma Rao D.V., Veda Bhanu G., 2001 “Design development and testing of Savonius wind turbine rotor with twisted blades” in Proceedings of 28th National Conference on Fluid Mechanics and Fluid Power, Chandigarh, India, 428 – 431
[12] Saha U.K., Jaya Rajkumar M., 2006, “On the performance analysis of Savonius rotor with twisted blades”, Renewable Energy 31:1776–1788
[13] Gupta R., Das R., Sharma KK., 2006, “Experimental study of a Savonius-Darrieus wind machine”, in proceedings of the International Conference on Renewable Energy for Developing Countries-2006
[14] Benghrib D., Ahram A., Bchir L., 1998, “Description de l'alternance des tourbillons d'un rotor Savonius par visualisation en tunnel hydrodynamique”, C. R. Acad. Sci. Paris, t. 326, Serie II b, 495-500
[15] Fujisawa N., 1996, “Velocity measurements and numerical calculations of flow fields in and around Savonius rotors”, J. Wind Eng. Ind. Aero., 59: 39-50
[16] Kawamura T., Hayashi T., Miyashita K., 2001, “Application of the domain decomposition method to the flow around the Savonius rotor”, in Proceedings of the 12th International Conference on Domain Decomposition Methods
[17] Menet J.-L., Bourabaa N., 2004, “Increase in the Savonius rotors efficiency via a parametric investigation”, in Proceeding of the European Wind Energy Conference, London, 22-24 November 2004
[18] Menet J.-L., Cottier F., 2003, “Etude paramétrique du comportement aérodynamique d'une éolienne lente à axe vertical de type Savonius”, Actes du 16 Congrès Français de Mécanique
[19] Shigetomia A., Murai Y., Tasakaa Y., Takedaa Y., “Interactive flow field around two Savonius turbines”, Renewable Energy, Volume 36, Issue 2, February 2011, Pages 536-545
[20] Cochran B.C., Banks D., Taylor S.J., 2004, “A Three-Tiered Approach for Designing and Evaluating Performance Characteristics of Novel WECS”; in Proceeding of the 42nd AIAA Aerospace Sciences Meeting and Exhibit, Reno, Nevada, Jan. 5-8, 2004
[21] D’Alessandro V., Montelparea S., Riccia R., Secchiarolia A., 2010, “Unsteady Aerodynamics of a Savonius wind rotor: a new computational approach for the simulation of energy performance”, Energy Volume 35, Issue 8, August 2010, Pages 3349-3363
[22] Le Gourieres D., 1982, “Wind Power Plant, Theory & Design”, Pergamon Press, New York, U.S.A.
[23] Wilcox D.C., "Turbulence Modeling for CFD",DCW Industries, 1993, ISBN: 0963605100